# A Design Approach For Planar Waveguide Launching Structures

J. Thornton, C. M. Mann.
Rutherford Appleton Laboratory, Chilton, Didcot, OX11 0QX, UK.

## Abstract

It is now possible to replace the conventional wire whisker with one that can be fabricated using lithographic techniques. This allows the device designer to implement a more ideal waveguide launching structure as an integral part of the whisker. It is possible to choose the physical form of the structure to match that required by an analytical model, thus providing more accurate prediction of the circuit behaviour. This paper describes the implementation of this concept and preliminary results will be presented demonstrating how the circuit behaviour of a varactor tripler centred around 250 GHz can be accurately predicted.

## Introduction

In the push to realise a solid state receiver for space applications at 2.5THz the LO requirement is now the crucial issue. A single diode 2nd harmonic mixer is an attractive option as LO drive levels similar to a fundamental mixer (≈0.5 mW) are required at only half the frequency. Substantial power is now being reported from solid state LO chains around 300 GHz [1, 2] (≈ 6-8 mW) and similar levels could be expected at 400 GHz in the near future and a cascaded tripler, with an efficiency of ≈6% could provide the last multiplication step to 1.25THz.

Varactor diodes are being developed with their optimum performance in the terahertz region. If accurate comparisons are to be drawn between diode batches then it is essential that the samples can be mounted in a configuration which allows control of the embedding conditions with a high degree of accuracy and in such a way that the RF circuit can be optimised in a reproducible manner.

Until the advent of the planar whisker the contact to the diode was made via a whisker formed from a bent wire. This structure is very difficult to accurately model, and in addition has to be made by hand which introduces fabrication errors. Since the whisker forms the main radiator within the cavity, small errors can have large effect on the device overall performance. The use of a lithographically produced 'flat' whisker frees the designer of many of the constraints associated with its wire predecessor. In particular, the radiating part of the whisker can take any form and because of this it becomes possible to fabricate the whisker to fit more closely an analysis method rather

than derive a model for a particular whisker. It is this simple, but important, concept that forms the basis of the work described here.

## The Eisenhart and Khan Analysis

This analysis [3] has been referred to in numerous publications in the field of microwave device design and optimisation, but often it is the embedding circuit measuring technique developed by the authors that is of interest and not the analysis itself. The measuring technique has now been accepted as a valid method of in situ measurements of embedding impedance at lower frequencies. The analysis itself, however, has not been widely adopted for device design despite its apparent accuracy - this is particularly true for whiskered diode devices. The reason for this appears to be that the structure it describes is difficult to realise physically, particularly at sub-millimetre wavelengths.

The Eisenhart and Khan analysis determines the impedance across a gap in a circular post positioned anywhere within a waveguide of rectangular cross-section (figure 1). The gap may be between the post and a wall of the waveguide - in this instance the analysis determines the impedance between the end of the post and the waveguide.

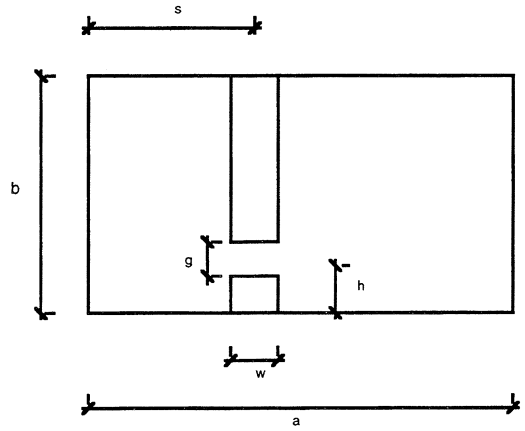


Figure 1. Geometry

a = waveguide width

b = waveguide height

s = post position (centre of post from side)

h = gap position (centre of gap from bottom)

g = gap size

w = post width

Also: s' = s / a normalised post position

h' = h / b normalised gap position

w' = w / a normalised post width

g' = g / b normalised gap size

The only restrictions on dimensions are that $w' < 0.25$ and $g' < 0.25$.

The analysis is valid for flat metallic posts, but approximates the behaviour for posts of circular cross section, the latter being the favoured mounting structure at the time of publication. This approximation has been removed since in our case the structure is planar in nature.

The theory behind the Eisenhart and Khan analysis is not discussed in detail here. However, a difficulty in verifying the analysis experimentally is that when a measurement is performed by placing a probe across the post gap (for example, at the end of a coaxial line), the gap impedance is modified by the reactance of the probe. The effect of this is described in [3] and was accounted for at the time by the addition of a simple circuit acting in shunt with the gap impedance. The equivalent circuit used in [3] is shown below:

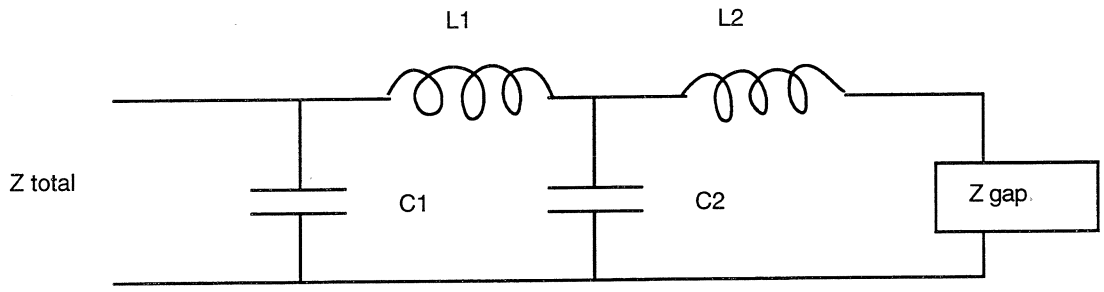


Figure 2. Equivalent circuit for measurement probe.

Where :

| | | |
|---|---|---|
| C1 = 15 $10^{-15}$ F | a = 4.760 cm | s and h are variable |
| C2 = 40 $10^{-15}$ F | b = 2.215 cm | |
| L1 = 360 $10^{-12}$ H | g = 0.153 cm | |
| L2 = 187 $10^{-12}$ H | w = 0.549 cm | |

The derivation of the above circuit is not described in detail by the original authors. However, by taking measurements on a waveguide model we have found that the values of the reactances were not constant for all post geometries, but were a function of w and g. In addition, it was found that the circuit could be further simplified to that shown in figure 3 and that the capacitance had very little effect on the modification of the gap impedance to that at the end of the probe.

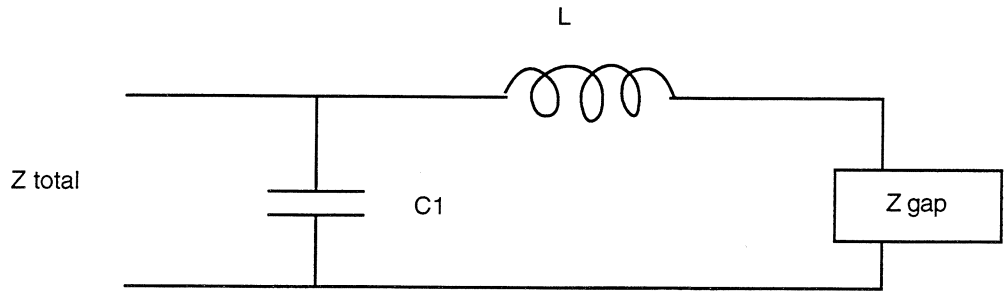


Figure 3. Simplified circuit for measurement probe.

C1 is the (shunt) fringing capacitance at the co-axial line termination.

L represents the sum of the series inductance of the probe and probe-post discontinuity.

The capacitance C1 may be approximated as the fringing capacitance of a coaxial line [5] and is constant for a given coaxial system. The circuit is dominated by the reactance of inductance L, which was derived empirically as a function of w and g (this is described in greater detail in [4].)

One of the powers of the analysis [3] is that the waveguide can be terminated in any complex reflection coefficient. This allows the inclusion of backshorts and idler circuits for example (see "Multiplier Modelling" below).

A simple computer model was written using *Mathematica* and various geometries of posts were compared with measured results obtained using the structure illustrated in figure 4 . This arrangement allowed the calibration plane of a network analyser to be moved as close as possible to the intended position for the diode in the actual device reducing phase errors due to the dispersion of dielectric-filled coaxial line. In addition, the scaled dimensions of the K connector aperture start to approach those of the diode anode used in the actual device.

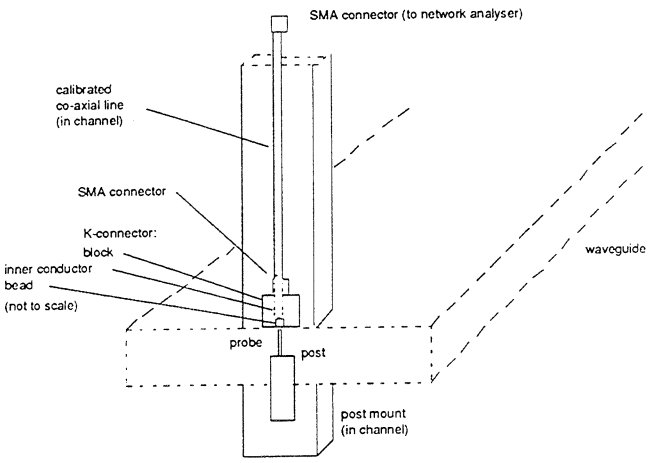


Figure 4. Measurement system for waveguide model.

Typical results shown below demonstrate the high level of agreement between the measured and computed cases. It should be noted that the value of probe inductance was varied empirically in the computer model until the best fit was obtained.

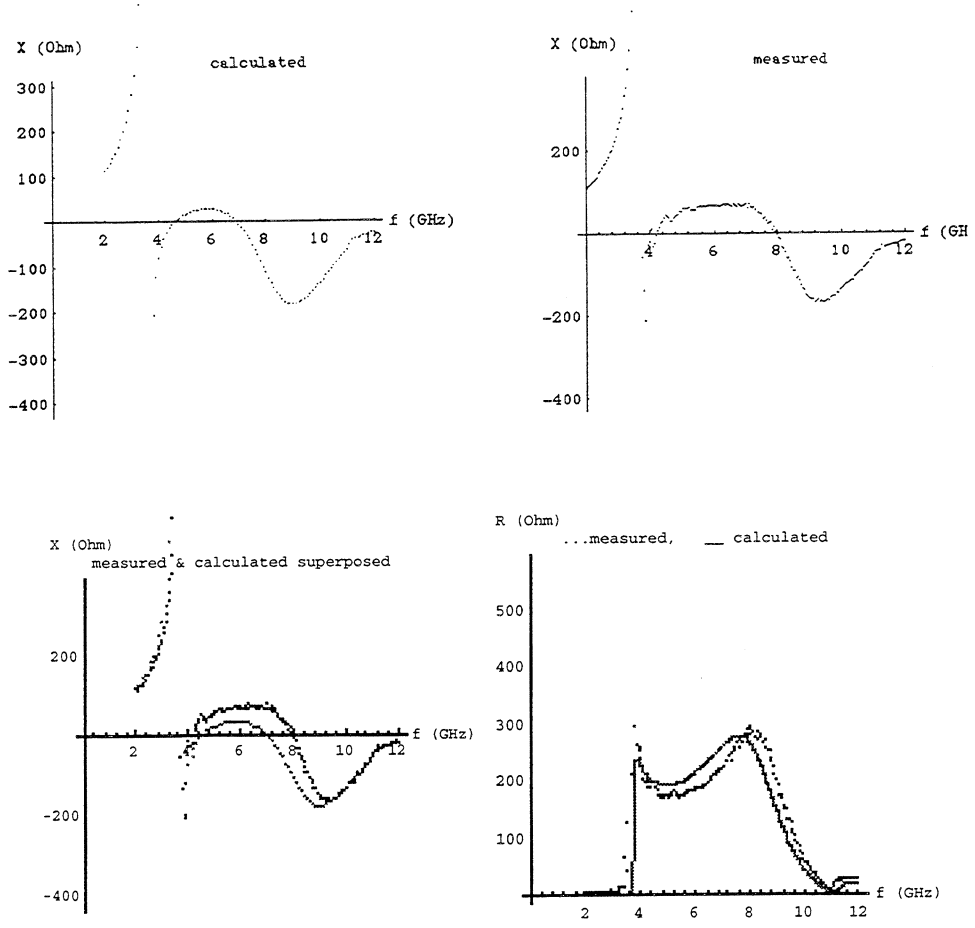


Figure 5(i). Comparison of computed and measured impedance.

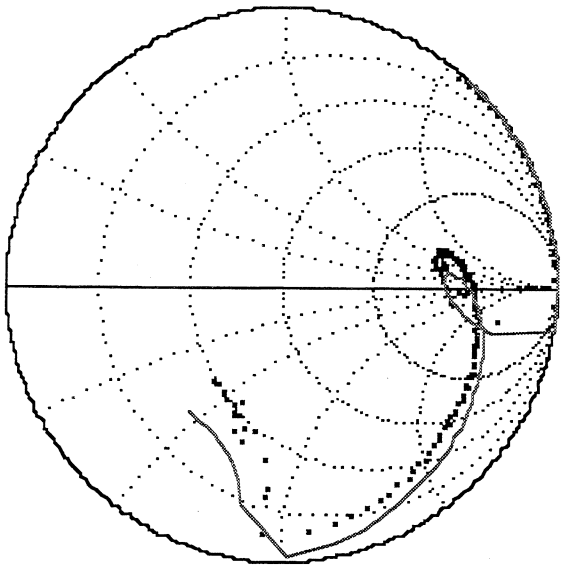

Smith chart plot ... measured __calculated

Dimensions: a = 40 mm, b = 10 mm, w = 4.0 mm, g = 2.2 mm, s = a/2, h = g/2.
Frequency: 2 GHz - 12 GHz (waveguide cut off frequency 3.7 GHz)
Figure 5(ii). Comparison of computed and measured impedance.

## Multiplier Modelling.

To test the level of agreement between the analysis and a device operating at millimetre wavelengths, a waveguide tripler was used. This had previously been assembled using conventional technology i.e. wire whiskers. The rectangular coupling probe required by the Eisenhart and Khan analysis was realised using a planar whisker ultrasonically bonded onto a gold post patterned using standard photolythographic techniques. This in turn was soldered onto a microstrip filter. A notch front X68 varactor diode (NMRC) was soldered onto the post that had previously carried the wire whisker. An SEM image of the assembled multiplier is shown below.

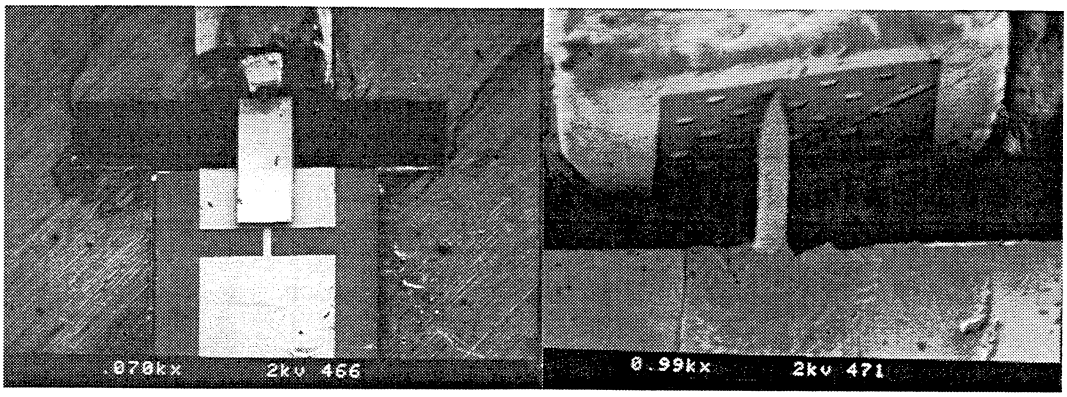


Figure 6. Assembled multiplier.

The physical dimensions of the post and waveguide, including the waveguide 2nd. harmonic idler length, were entered into the analysis program. Toward the output waveguide it was assumed that the 2nd. harmonic was terminated by a perfect short circuit at the position where the waveguide becomes cut-off. The 3rd and 4th harmonics were assumed to be terminated by matched loads. The other arm of the waveguide was terminated by the reflection coefficient of a perfect short circuit, for all harmonics considered, at the position of the backshort. The analysis was then performed for a range of backshort positions corresponding to the full extent of travel available in the actual device. An important practical feature of our method is that computing time is minimal when compared to other commercially available software that encompasses structures in waveguide. A full 'sweep' of the backshort (≈200 positions) takes in the region of 10-20 minutes to calculate the embedding impedances at 2nd, 3rd and 4th harmonics. The corresponding set of calculated embedding impedances for the three main harmonics of interest were obtained. These where then entered into a diode non-linear analysis programme [6] in order to produce a table of multiplier predicted power output as a function of backshort position. The actual tripler was then measured to allow comparison and the results, which were very encouraging, are shown in figure 7 below.

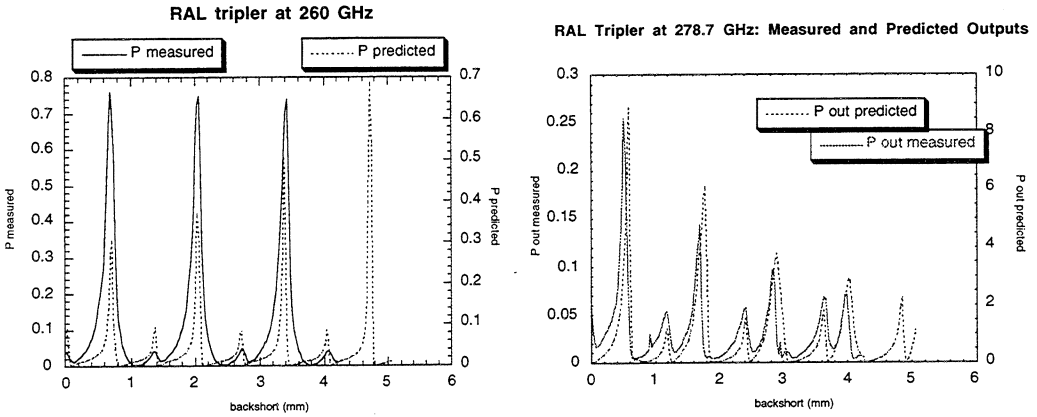


Figure 7. Comparison of measured and predicted tripler performance.

To understand the structure shown in the backshort response it is necessary to consider the embedding impedances presented to the diode as the backshort is moved. Essentially, the embedding impedances at the different harmonics are changing at different rates set by the guide wavelength in each case. A plot of predicted output power as a function of embedding impedance can be conveniently shown on a Smith chart, for each harmonic independently. A series of contours appear to be drawn, centred around an optimum value. An example is shown in figure 8 below which shows a typical form for the output harmonic impedance of a multiplier [7]. The efficiencies shown are relative to the optimum condition.

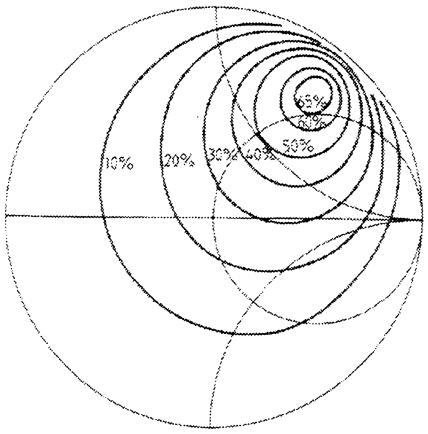


Figure 8. Typical performance contours as a function of impedance at output frequency.

As the backshort is moved the embedding impedance for each harmonic crosses these contours. At the point where the combined harmonic contribution to the third is at a maximum, a peak in the output power is observed for that particular backshort position. Because of the different guide wavelengths for each harmonic, each peak moves in relation to the next and the magnitude of the output power varies between successive peaks.

This effect is seen most clearly in the results at 279 GHz. The major peaks are observed to decrease in magnitude; this might be attributed to excessive waveguide loss until it is observed that at the same time the minor peaks increase in magnitude.

The best agreement for the shape of the curves occurred for the higher frequencies, whereas at 250 GHz (first plot figure 8) the agreement is virtually non existent. This becomes understandable when the behaviour of the microstrip filter is taken into account. In deriving these curves it is assumed that there is a perfect short between the end of the probe and the waveguide wall. However, in the actual device the end of the probe is attached to the microstrip filter which, while providing very nearly a pure reactance to the probe, exerts a phase change which varies as a function of frequency. The good agreement at 260 and 279 GHz is attributed to the filter presenting an impedance that is very close to that of a short circuit for the 2nd and 3rd harmonics simultaneously, but this condition cannot be satisfied at all frequencies.

To investigate this effect further, the predicted backshort response at 250 GHz was derived again but using phase-modified impedances i.e. different phase offsets were applied to the impedances at the second, third and fourth harmonics until a much improved agreement was observed, as shown in the second plot of figure 9. The phase changes introduced were comparable with those expected from a simple transmission

line model of the filter, which suggests that the method can be enhanced by a further understanding of filter behaviour.

It is particularly interesting to note that at 250 GHz the combined analyses also show the "noisy" structure on the broad peaks which prior to the correction for the phase error introduced by the filter had been put down to a poorly contacting backshort whereas in actual fact it is a real effect that can be attributed to the electrical behaviour of the mount.

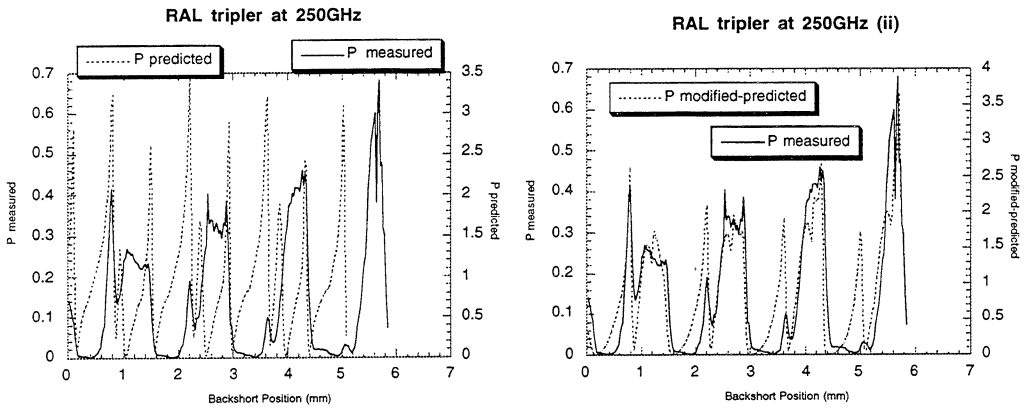


Figure 9. Comparison of measured tripler performance and prediction using phase-modified embedding impedance.

## Multiplier Performance.

The ultimate aim of this work is to obtain higher power outputs and efficiencies from frequency multipliers. Examination of the previous results shows that the predicted and measured output powers are very different. Whilst initially disappointing, it should be noted that there are a number of reasons that reduce power levels. Firstly, whilst moving the output waveguide backshort it is not desirable to re-tune the input backshorts as these partially act on embedding impedance at the diode independently of the output backshort, an effect which cannot be accounted for in the analysis. Consequently the output powers shown do not reflect a true absolute value but one lower than that which could be obtained for any given output backshort position. Secondly, the power applied to the input has to be kept at a low level to avoid peak currents at certain positions of the output from becoming excessive and burning out the diode. Thirdly, no account is taken for power reflected at the input - ideally the results should be normalised for incident power at the diode rather than power at the waveguide input port. The input power used in the Seigel and Kerr analysis was kept at a constant nominal value of 50 mW for all cases. The power output predicted is a function of how the Seigel and Kerr analysis uses the values of embedding impedance coupled to the non-linear diode model, via the harmonic balance technique. It is unlikely that the model for the diode used in our version of the analysis completely describes the

true diode behaviour at these frequencies. In particular it is now known that the series resistance is a function of applied voltage and is therefore non-linear whereas in the version used here the series resistance is considered constant. Also, no account is taken for the loss within the waveguide mount itself.

At a given harmonic there is a single optimum value of embedding impedance, deviations from which lead to reduced power for each harmonic under consideration, the first through to the third being dominant in the case of a tripler. Other factors governing performance include the filter efficiency, diode series resistance and the effectiveness of the backshort in the device, which are now the subject of separate studies.

This work is now being continued and the results to date have given valuable insight into the multiplication mechanism within a working device. Before this study, the tripler mount designed and empirically optimised using a conventional wire whisker would give between 1.5 and 2 mW of power at saturation. Recent modifications based on improvements suggested by this analysis technique have lead to the same device producing 4.75 mW at saturation at the same frequency i.e. 270 GHz. This result was obtained using a 5M4 varactor diode from UVA. For continuous operation the device will routinely provide 4 mW of power. When power output was kept to a conservative 2.0 mW, the multiplication efficiency at 242 GHz was 5.8 % (allowing for reflected power at the input)

The improvement in the performance of the device studied is practical evidence of the validity of this approach. Further investigation has suggested shortcomings in this intermediate design and a full optimisation of the device design and mount should yield further improvements in the near future. The final step in the process is to correlate this analysis with an improved model for the varactor diode in order to optimise the diode design and waveguide mount simultaneously.

**Acknowledgement.**

The authors would like to express thanks to Dr. P. de Maagt of ESTEC for his support and interest in this work.

**References.**

[1] 'Frequency Multipliers and LO sources for the Submillimetre wave Region', P. Zimmermann, Proc. ESA Workshop on Millimetre wave Tech. and Appl. ESTEC, Noordwijk, Dec. 1995.

[2] 'Novel Planar Varactor Diodes', P.J. Koh, W.C.B. Peatman, T.W. Crowe, Neal R. Erickson, 7th Int. Symp. Space THz Technology, Charlottesville, March 96.

[3] 'Theoretical and Experimental Analysis of a Waveguide Mounting Structure', R.L.Eisenhart, P.J.Khan , IEEE Transactions on Microwave Theory and Techniques VOL. MTT-19 no.8 August 1971.

[4] 'Embedding Impedance of Waveguide Diode Mounting Structures', J.Thornton, Project Report for MSc. in Microwave Solid State Physics, University of Portsmouth, UK. October 1995.

[5] 'Waveguide Handbook', N.Marcuvitz (IEE Electromagnetic Waves Series 21), pp 213 - 216.

[6] 'Topics in the Optimisation of Millimetre Wave Mixers', P. H. Siegel, A.R. Kerr, W. Hwang, NASA Technical Paper 2287, March 1984.

[7] 'An Efficient Schottky-Varactor Frequency Multiplier at Millimetre Waves', Part 1: Doubler, T.J.Tolmunen, A.V.Räisänen, International Journal of Infrared and Millimetre Waves, Vol.8 No.10, Oct 1987.